FcγRII/III and CD2 Expression Mark Distinct Subpopulations of Immature CD4$^-$CD8$^-$ Murine Thymocytes: In Vivo Developmental Kinetics and T Cell Receptor β Chain Rearrangement Status

By Hans-Reimer Rodewald,*‡ Katherine Awad,* Philippe Moingeon,*‡ Luciano D'Adamio,*‡ Daniel Rabinowitz,‖ Yoichi Shinkai,¶ Frederick W. Alt,¶ and Ellis L. Reinherz*§

*From the *Laboratory of Immunobiology, Dana-Farber Cancer Institute and Departments of ‡Pathology and §Medicine, Harvard Medical School; the ‖Department of Biostatistics, Harvard School of Public Health; and ¶The Howard Hughes Medical Institute, The Childrens Hospital, Boston, Massachusetts 02115*

Summary

We have recently identified a dominant wave of CD4$^-$CD8$^-$ (double-negative [DN]) thymocytes in early murine fetal development that express low affinity Fcγ receptors (FcγRII/III) and contain precursors for Tiα/β lineage T cells. Here we show that FcγRII/III is expressed in very immature CD4^{low} single-positive (SP) thymocytes and that FcγRII/III expression is downregulated within the DN subpopulation and before the CD3$^-$CD8^{low} SP stage in T cell receptor (TCR)-α/β lineage-committed thymocytes. DN FcγRII/III$^+$ thymocytes also contain a small fraction of TCR-γ/δ lineage cells in addition to TCR-α/β progenitors. Fetal day 15.5 DN TCR-α/β lineage progenitors can be subdivided into three major subpopulations as characterized by cell surface expression of FcγRII/III vs. CD2 (FcγRII/III$^+$CD2$^-$, FcγRII/III$^+$CD2$^+$, FcγRII/III$^-$CD2$^+$). Phenotypic analysis during fetal development as well as adoptive transfer of isolated fetal thymocyte subpopulations derived from C57Bl/6 (Ly5.1) mice into normal, nonirradiated Ly5.2 congenic recipient mice identifies one early differentiation sequence (FcγRII/III$^+$CD2$^-$ → FcγRII/III$^+$CD2$^+$ → FcγRII/III$^-$ CD2$^+$) that precedes the entry of DN thymocytes into the CD4$^+$CD8$^+$ double-positive (DP) TCR$^{low/-}$ stage. Unseparated day 15.5 fetal thymocytes develop into DP thymocytes within 2.5 d and remain at the DP stage for >48 h before being selected into either CD4$^+$ or CD8$^+$ SP thymocytes. In contrast, FcγRII/III$^+$CD2$^-$ DN thymocytes follow this same developmental pathway but are delayed by ~24 h before entering the DP compartment, while FcγRII/III$^-$CD2$^+$ display accelerated development by ~24 h compared with total day 15.5 thymocytes. FcγRII/III$^-$CD2$^+$ are also more developmentally advanced than FcγRII/III$^+$CD2$^-$ fetal thymocytes with respect to their TCR β chain V(D)J rearrangement. At day 15.5 in gestation, β chain V(D)J rearrangement is mostly, if not entirely, restricted to the FcγRII/III$^-$CD2$^+$ subset of DN fetal thymocytes. Consistent with this analysis in fetal thymocytes, >90% of adult thymocytes derived from mice carrying a disrupting mutation at the recombination-activating gene 2 locus (RAG-2$^{-/-}$) on both alleles are developmentally arrested at the DN CD2$^-$ stage. In addition, there is a fivefold increase in the relative percentage of thymocytes expressing FcγRII/III in TCR and immunoglobulin gene rearrangement–incompetent homozygous RAG-2$^{-/-}$ mice (15% FcγRII/III$^+$) versus rearrangement-competent heterozygous RAG-2$^{+/-}$ mice (<3% FcγRII/III$^+$). Thus, FcγRII/III expression defines an early DN stage preceding $V_\beta(D_\beta)J_\beta$ rearrangement, which in turn is followed by surface expression of CD2. Loss of FcγRII/III and acquisition of CD2 expression characterize a late DN stage immediately before the conversion into DP thymocytes.

 J. Exp. Med. © The Rockefeller University Press • 0022-1007/93/04/1079/14 $2.00
Volume 177 April 1993 1079–1092

T lymphocytes develop in the thymus from fetal liver or adult bone marrow–derived progenitor cells that colonize the fetal thymus continuously beginning around day 12 in the development of the mouse (1, 2). Progenitor activity giving rise to both T cell (Tiα/β and Tiγ/δ) lineages has been identified in the $CD4^-CD8^-$ double-negative (DN)[1] population of thymocytes (reviewed in references 3–6). DN thymocytes represent the major population in the early fetal thymus (~95% at day 15.5 in gestation of the mouse) and are reduced to ~5% in the adult thymus due to the presence of more developed thymocytes. TCR-α/β lineage thymocytes begin to rearrange their TCR genes at the DN stage (7–9) and pass through a $CD3^-CD8^{low}$ (10, 11) stage into the $CD4^+CD8^+$ double-positive (DP) $TCR^{low/-}$ stage. On the basis of their TCR specificity, DP thymocytes are selected into $CD4^+$ or $CD8^+TCR^{high}$ single-positive (SP) mature thymocytes that populate the peripheral lymphoid organs (reviewed in reference 12).

We have recently identified a wave of DN thymocytes in early fetal development (day 14.5 in gestation) that express Fc receptors for IgG (FcγRII/III) (13). Intrathymic transfer of purified fetal DN FcγRII/III$^+$ thymocytes demonstrated the Tiα/β lineage progenitor activity of these cells. Developmental progression included the conversion from the $CD3^-CD4^-CD8^-$FcγRII/III$^+$ stage to the $CD3^+CD4^+CD8^+$ stage and the subsequent selection into CD4 or CD8 SP mature T cells. Of note, FcγRII/III expression was shown to be downregulated between the DN and DP stages. However, $CD3^-CD4^-CD8^-$FcγRII/III$^+$ thymocytes also contained precursor activity for the generation of NK cells. This property became apparent upon removal of fetal thymocytes from the thymus and subsequent in vitro culture in the presence of IL-2 or upon intravenous transfer into recipient mice. In contrast to the loss of FcγRII/III expression during intrathymic development, FcγRII/III expression was maintained on cellular progeny derived from $CD3^-CD4^-CD8^-$FcγRII/III$^+$ cells outside the thymus (13).

While the percentage of FcγRII/III-expressing thymocytes declines during early fetal development, the number of CD2-expressing thymocytes increases (14, 15). The early onset of CD2 expression (day 14 in gestation) in developing thymocytes led to the speculation that CD2-mediated adhesion and/or signaling might play a role in thymus-specific differentiation (16). Furthermore, the loss of FcγRII/III expression and the acquisition of CD2 expression during early T cell ontogeny suggest that there are additional developmentally and phenotypically distinct subpopulations of DN thymocytes just before the transition into the DP stage. Here we report on the identification of such distinct subsets of DN thymocytes as defined by their expression of FcγRII/III and CD2, their TCR β chain rearrangement status, and their in vivo differentiation kinetics in normal recipient mice. The elucidation of this developmental sequence within DN thymocytes is entirely consistent with the differentiation block that occurs in TCR gene rearrangement–incompetent animals whose RAG-2 genes (17, 18) have been disrupted on both alleles (19). Moreover, analysis of $CD3^-CD4^-CD8^-$ thymocytes from adult mice identified the same phenotypic stages as found among fetal thymocytes, suggesting that these subpopulations of DN thymocytes are part of a functional developmental pathway in the adult thymus as well. Finally, while the majority of the DN FcγRII/III$^+$ subset are apparently TCR-α/β progenitors, a small fraction of DN FcγRII/III$^+$ thymocytes enter the TCR-γ/δ lineage.

[1] *Abbreviations used in this paper:* DN, double negative; DP, double positive; HSA, heat-stable antigen; RAG-2, recombination-activating gene 2; SP, single positive.

Materials and Methods

Mice. C57Bl/6 (Ly5.1) mice were obtained from The Jackson Laboratory (Bar Harbor, ME) and breeding stocks of the congenic strain B6Ly5.2 (Ly5.2) were kindly provided by Dr. Clarence Reeder (National Cancer Institute, Frederick, MD) and maintained at the Redstone Animal Facility at the Dana-Farber Cancer Institute (Boston, MA). Thymocytes were isolated from fetal mice that were obtained from timed pregnant C57Bl/6 mice. The day of the vaginal plug was counted as day 1 of pregnancy. RAG-$2^{-/-}$ and RAG-$2^{+/-}$ mice (19) were kept under specific pathogen-free conditions.

mAbs. The following primary antibodies were used in this study: biotinylated 2.4G2, FITC-conjugated 2.4G2 (20), PE-coupled 53-2.1 (21) (anti-Thy-1; Gibco BRL, Gaithersburg, MD), FITC-conjugated M1/69 (22) (anti-HSA; Pharmingen, San Francisco, CA), biotinylated 7D4 (23) (anti-IL-2R [p55]), biotinylated RM2-1 (24) (anti-CD2; Pharmingen), control antibody Y13-238 (25) (anti-p21 ras), PE-coupled YCD3-1 (26) (anti-CD3; Gibco BRL), FITC-labeled 145-2C11 (anti-CD3) (27), FITC-labeled 3A10 (anti-pan Tiγ/δ) (28) PE-coupled GK1.5 (29) (anti-CD4; Becton Dickinson & Co., Mountain View, CA), biotinylated 53-6.7 (21) (anti-CD8; Becton Dickinson & Co.), Red613-coupled 53-6.7 (anti-CD8; Gibco BRL), PE-coupled RA3-6B2 (30) (anti-B220; Caltag, San Francisco, CA), allele-specific FITC-conjugated 104-2.1 (anti-Ly5.1) (31), FITC-labeled A20-1.7 (anti-Ly5.2) (31). Both hybridomas were kindly provided by Dr. S. Kimura (Sloan-Kettering Cancer Center, New York). Second-step reagents were streptavidin-PE and streptavidin-FITC (Tago Inc., Burlingame, CA). mAbs were grown as culture supernatants and depending on the species and isotype purified on protein A– or protein G–Sepharose (Pharmacia LKB, Uppsala, Sweden). mAbs were biotinylated using NHS-LC-Biotin (Pierce Chemical Co., Rockford, IL) following the manufacturer's recommendations and FITC labeled using fluorescein-5-isothiocyanate (FITC Isomer I; Molecular Probes, Eugene, OR) using standard procedures (32). Following the labeling procedures, specific reactivity of mAbs was analyzed by FACS® (Becton Dickinson & Co.) and the optimal antibody dilutions were subsequently used.

Immunofluorescence Staining, Analysis, and Cell Sorting. For phenotypic analysis, thymocytes were obtained from normal fetal mice at different days of timed pregnancies, or at the indicated times after cell transfer into recipient mice, and stained with mAbs as indicated in the figure legends. 0.5–1 × 10^6 cells from single-cell suspensions were incubated with purified mAbs at 5–10 μg/ml in PBS, 5% FCS for 15–30 min on ice, washed in PBS, 5% FCS and, if necessary, incubated with the appropriate second-step reagents for 15–30 min on ice. Flow cytofluorometric analysis was performed on a FACScan® (Becton Dickinson & Co.). In experiments shown in Figs. 1–3, 6, and 7, 10^4 cells were analyzed. For reanalysis of donor-type cells (summarized in Fig. 4 *B*), 5 × 10^4 cells were analyzed, in each case gating on viable cells by forward angle and sideward scattering properties. Fluorescence data are displayed as loga-

rithmic overlay histograms, contour, or dot plots using LYSYS software (Becton Dickinson & Co.).

For cell sorting, fetal thymocytes derived from timed pregnant C57Bl/6 mice (day 15.5) were stained with 2.4G2-FITC (10 μg/ml) and CD2-biotin (1:50 dilution) followed by avidin-PE (1:50 dilution) and separated into $CD2^+$ $Fc\gamma RII/III^-$ and $CD2^-$ $Fc\gamma RII/III^+$ subpopulations at a flow rate of 1,500 cells/s using an EPICS 750 series cell sorter (Coulter Electronics, Hialeah, FL). Sorted cell populations were reanalyzed for their purity and were found to be at least 97% pure. For control purposes, fetal day 15.5 thymocyte (FT day 15.5) total cells were stained with 2.4G2-FITC (10 μg/ml) and CD2-biotin (1:50 dilution), followed by avidin-PE, but not separated before intrathymic injection.

Enrichment of $Ly5.1^+$ Cells through Magnetic Bead Separation. For enrichment of $Ly5.1^+$ cells from Ly5.2 recipient mice, thymocytes were incubated with purified A20-1.7 (anti-Ly5.2) at 10 μg/ml for 30 min on ice and washed in PBS, 5% FCS. Magnetic goat anti-mouse IgG beads (Advanced Magnetics, Cambridge, MA) were washed twice by placing the magnetic bead suspension between two strong magnets, removing liquid, and resuspending beads in PBS, 5% FCS. Thymocytes were then incubated with magnetic beads (1 ml magnetic bead suspension/10^7 cells) for 30 min on ice. To remove $Ly5.2^+$ cells bound to magnetic beads, the suspension was placed between two magnets until fluid was clear (~5 min). Fluid, enriched in $Ly5.1^+$ cells, was then removed and again incubated with an equivalent amount of magnetic beads for 30 min on ice. For the final separation, the suspension was placed between magnets and the transparent fluid removed. This last step was repeated three times to obtain maximum enrichment of $Ly5.1^+$ cells. This procedure yielded 5–50-fold enrichment of donor-type cells relative to host cells. In general, 50–500 (0.1–1%) donor-type cells were observed per 5×10^4 total thymocytes analyzed with no significant difference detected when comparing the cell numbers of progeny of the injected DN $Fc\gamma RII/III^+CD2^-$ and DN $Fc\gamma RII/III^-CD2^+$ subpopulations.

Isolation of Adult $CD3^-CD4^-CD8^-$ Thymocytes. To prepare adult $CD3^-CD4^-CD8^-$ thymocytes, normal adult thymocytes were incubated at a concentration of 2×10^7/ml with PE-coupled GK1.5 (10 μg/ml) and biotinylated 53-6.7 (10 μg/ml) for 30 min on ice. After extensive washing the cells were resuspended at a concentration of 10^7/ml with magnetic goat anti-rat IgG beads (Advanced Magnetics) at a ratio of 10–50 particles/cell and incubated for 30 min on ice. $CD4^+$ and $CD8^+$ thymocytes binding to magnetic beads were subtracted using two magnets (Advanced Magnetics) as described above. The latter step was repeated twice. By this time, $CD4^-$ and $CD8^-$ thymocytes were enriched to ~60%. To further purify the DN population and to remove DN $CD3^+$ cells, the remaining cell population was restained with PE-coupled GK1.5 (10 μg/ml), biotinylated 53-6.7 (10 μg/ml), and PE-coupled YCD3-1 for 30 min on ice, washed, and subsequently incubated with streptavidin-PE. PE-negative thymocytes (corresponding to $CD3^-CD4^-CD8^-$ thymocytes) were sorted on an EPICS 750 series cell sorter (Coulter Electronics). Postsorter analysis showed the purity of the sorted population to be >97%.

Intrathymic Injections. Intrathymic injections were performed as described (13, 33, 34). Briefly, 4–6-wk-old mice were anesthetized with Avertin (2.5% solution, 10 μl per gram body weight) as described (35) and injected intrathymically without prior irradiation. For injections, mice were positioned on their back, a small incision (<5 mm) was made in the skin above the sternum without opening the thorax, and cells were injected into each thymic lobe by positioning the needle for injection from cranio-lateral to caudo-medial and injecting through the thorax wall above the clavicle. Cells (10^5/thymus) were injected using a 1-ml syringe (Insulin Syringe; Becton Dickinson & Co., Rutherford, NJ) placed into a stepper (Tridak, Brookfield, CT) in 20 μl PBS with 5% FCS per lobe. Subsequently, the skin wound was closed using surgical metal clips.

Template Preparation for PCR Analysis. Genomic DNA from various tissues was isolated from C57Bl/6 mice. Single-cell suspensions from fetal liver, fetal thymus, and adult lymph nodes were washed in cold PBS, resuspended in cold PBS, 0.5% NP-40, and incubated on ice for 15 min. Nuclei were spun down, resuspended in 0.5 ml TNE (50 mM Tris, 100 mM NaCl, 1 mM EDTA) with 0.5 mg/ml proteinase K and 1% SDS, and incubated overnight at 37°C. Genomic DNA was extracted once with TE-saturated phenol and once with chloroform and precipitated with 0.3 M NaOAc (pH 5.9) and ethanol.

PCR and Southern Hybridization Analysis. PCR was carried out as described (36). In brief, we used ~100 ng (or dilutions thereof) of DNA template, 5 pmol of primers Jβ2.5 (5′-TAACACGACGAGCCGAGTGC-3′) and Vβ6 (5′-GAAGGCTATGATGCGTCTCG-3′), 10 pmol of primer Vβ8 (5′-TCCCTGATGGGTACAAGGCC-3′), and 1 U of taq polymerase (Perkin Elmer Cetus, Norwalk, CT) in 50 μl final volume. The samples were denatured (94°C, 1 min), annealed (64°C, 1 min) and extended (72°C, 30 s) for 35 cycles. Aliquots from each sample were size fractionated on a 1.5% Tris-borate-EDTA agarose gel, denatured in 0.25 M HCl, and blotted onto a zeta probe membrane (Bio-Rad Laboratories, Richmond, CA) in 0.4 M NaOH. Blots were then hybridized with a Jβ2.5-specific oligonucleotide probe (5′-CTGGCCCAAAGTACT GGGTG-3′) using standard methods (36).

To control the integrity and amount of genomic DNA templates, a genomic sequence within exon 8 of CD3ζ was amplified using the sense oligonucleotide (5′-CAGACCCTGGCC CCTCGC-3′) and the antisense oligonucleotide (5′-GCTACCCCAGGCTCACCAC-3′). The samples were denatured (94°C, 1 min), annealed (62°C, 1 min), and extended (72°C, 1.5 min) for 35 cycles. Blots were hybridized with a CD3ζ exon 8–specific oligonucleotide probe (5′-GGGCTTCACCTGCTGATGTC-3′). All oligonucleotides were made on a synthesizer (381A; Applied Biosystems, Inc., Foster City, CA) using standard β-cyanoethylphosphoramidate chemistry.

Statistical Analysis. To determine the statistical significance of kinetic differences in the development of various fetal thymocyte populations 1.5–7.5 d postintrathymic injection as measured in the experiments summarized in Fig. 4 *B*, a permutation test (37) was used to determine the difference between the control population (FT day 15.5 total) and either $Fc\gamma RII/III^+CD2^-$ or $Fc\gamma RII/III^-CD2^+$. The test statistic used was the sum, over times, of the squares of the differences between the sample averages of the percentages. The permutations were the relabelings of group identity that fixed the number of observations at each time and in each group (with $p < 0.001$).

Results

Expression of FcγRII/III on Fetal Thymocytes Is Restricted to Immature $CD4^{low}CD8^-$ and DN Stages. To examine the expression of FcγRII/III on subpopulations of developing thymocytes, FT day 17.5 were analyzed for surface expression of CD4, CD8, and FcγRII/III by three-color immunofluorescence (Fig. 1, *A* and *B*). FT day 17.5 was chosen for this analysis because this developmental stage displays three distinct immature thymocyte populations expressing CD4 and CD8 differentially: DN, $CD3^-$ $CD8^{low}$ SP, and DP

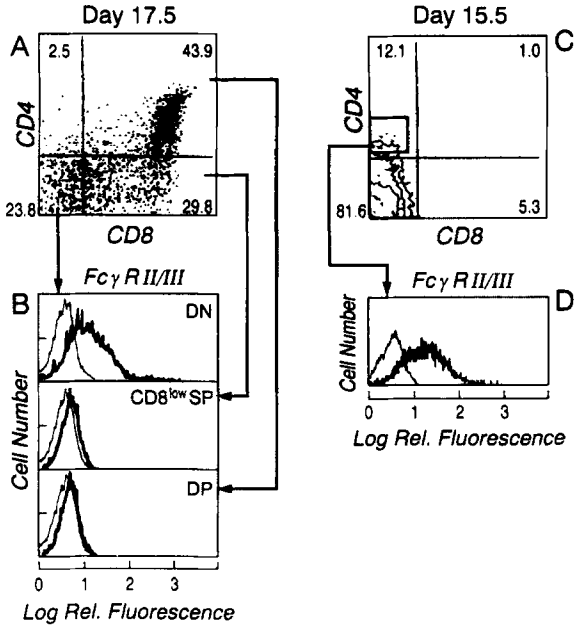

Figure 1. FcγRII/III expression on CD4⁻CD8⁻ (DN) and CD4^{low}CD8⁻ thymocytes during early fetal development. Fetal thymocytes derived from timed pregnant CD57Bl/6 mice at day 17.5 (*A* and *B*) or day 15.5 (*C* and *D*) of gestation were analyzed by three-color flow cytometry for the expression of CD4, CD8, and FcγRII/III. Overlay histograms (*B* and *D*) display FcγRII/III expression of gated thymocytes populations (*A* and *C*). FcγRII/III expression on CD4⁻CD8⁻ (DN), CD4⁻CD8^{low} (CD8^{low}SP), and CD4⁺CD8⁺ (DP) subpopulations is shown in *B*, and on the CD4^{low}CD8⁻ subset in *D*. Overlay histograms represent specific staining of a gated subpopulation with FITC-labeled 2.4G2 (anti-FcγRII/III) (*bold lines*) vs. staining of the same subpopulation with FITC-labeled 2.4G2 after preincubation with excess of unlabeled 2.4G2 (*thin lines*).

subsets. Gated subpopulations of DN, CD8^{low} SP, and DP (Fig. 1 *A*) were analyzed for their expression levels of FcγRII/III. This analysis revealed the highest expression of FcγRII/III on the DN population, while both immature CD8^{low} SP and DP thymocytes are FcγRII/III⁻ (Fig. 1 *B*). Overlay histograms shown in Fig. 1 *B* compare specific staining of thymic subpopulations with FITC-labeled mAb 2.4G2 (*bold lines*) vs. 2.4G2-FITC staining of the same subpopulations after preincubation with an excess of unlabeled 2.4G2 (*thin lines*). This expression pattern is consistent with our previous observation of a parallel decline in the percentage of DN and FcγRII/III⁺ fetal thymocytes during gestation in situ as well as the loss of FcγRII/III on adoptively transferred FcγRII/III⁺ DN T cell progenitors during their development from the DN to the DP stage in the thymus (13).

The above results indicated that FcγRII/III expression is found at the DN stage and lost before further differentiation. To analyze FcγRII/III expression on yet earlier intrathymic progenitor cells, we examined the 2.4G2 reactivity on the recently described CD4^{low} SP immature population, which precedes the DN stage (38, 39). Three-color immunofluorescence analysis on FT day 15.5 for CD4, CD8, and FcγRII/III (Fig. 1 *C*) revealed that FcγRII/III was also expressed on the majority of the CD4^{low} SP immature population (Fig. 1 *D*). This finding indicates that a very early intrathymic T cell progenitor population expresses FcγRII/III.

Several Distinct Subpopulations of DN Fetal Thymocytes Are Defined during Early Development by FcγRII/III Expression. DN thymocytes can be subdivided into phenotypic subpopulations by expression of a number of cell surface proteins (40, 41), i.e., the IL-2R α chain (p55) (34, 42), the levels of expression of Thy-1 (43), heat-stable antigen (HSA) (44, 45), and CD2 (14, 15). To analyze the presence or absence of these early stage-related markers on FcγRII/III⁺ and FcγRII/III⁻ thymocyte populations, thymocytes derived from days 14.5, 15.5, and 16.5 of fetal development, respectively, were stained for expression of FcγRII/III vs. Thy-1 (Fig. 2 *A*), IL-2R (p55) (Fig. 2 *B*), CD2 (Fig. 2 *C*), and HSA (Fig. 2 *D*). This analysis reveals heterogeneity among FcγRII/III⁺ and FcγRII/III⁻ thymocytes. While the majority of FcγRII/III⁺ thymocytes at day 14.5 are Thy-1^{high} and HSA^{high} (Fig. 2, *A* and *D*, *top*), a minority of FcγRII/III⁺ thymocytes express medium to low levels of Thy-1 and HSA. As has been described previously, the number of FcγRII/III⁺ thymocytes drastically declines during fetal development (13). However, the expression levels of Thy-1 and

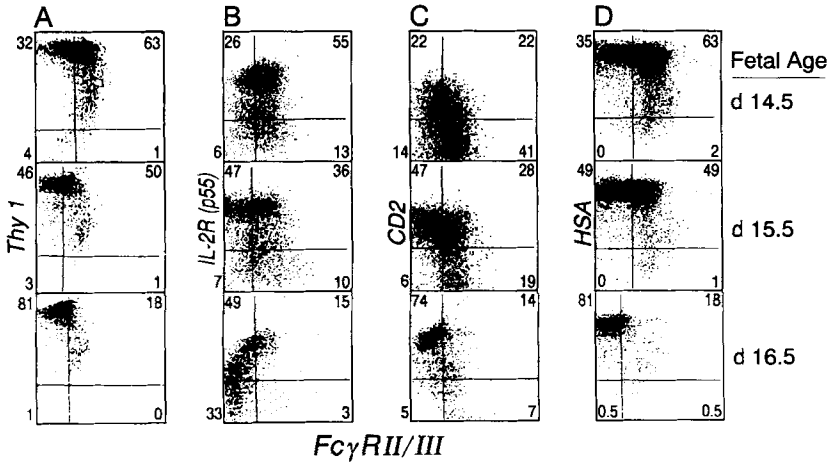

Figure 2. Several distinct subpopulations of fetal thymocytes are defined during early fetal development by FcγRII/III expression. Fetal thymocytes derived from timed pregnant C57Bl/6 mice at days 14.5, 15.5, and 16.5 of gestation were analyzed by flow cytometry for expression of FcγRII/III vs. Thy-1 (*A*), IL-2R α chain (p55) (*B*), CD2 (*C*), and HSA (*D*). Note the downregulation of FcγRII/III expression during this early stage of thymic development while the expression levels of Thy-1 and HSA remain high (*A* and *D*). The loss of FcγRII/III expression appears to precede the loss of IL-2 R (p55) expression (*B*). Analysis of cell surface expression of FcγRII/III vs. CD2 (*C*) suggests an early developmental sequence involving the following phenotypic stages of DN thymocytes: FcγRII/III⁺CD2⁻ → FcγRII/III⁺CD2⁺ → FcγRII/III⁻CD2⁺.

HSA remain high during the FcγRII/III downregulation (Fig. 2, *A* and *D*). In contrast, analysis of developing thymocytes for FcγRII/III vs. IL-2R (p55) (Fig. 2 *B*) reveals a major population of predominantly FcγRII/III$^+$ IL-2R (p55)$^+$ day 14.5 thymocytes and a minor population of FcγRII/III$^+$ IL-2R (p55)^{low} day 14.5 thymocytes (Fig. 2 *B*, *top*). The loss of FcγRII/III appears to precede the loss of IL-2R (p55) on day 15.5 fetal cells (Fig. 2 *B*, *middle*), before thymocytes enter a FcγRII/III$^-$ IL-2R (p55)$^-$ stage on day 16.5 (Fig. 2 *B*, *bottom*). Analysis of cell surface expression of FcγRII/III vs. CD2 (Fig. 2 *C*) demonstrates that the majority of FcγRII/III$^+$ thymocytes at day 14.5 are CD2$^{low/-}$ (Fig. 2 *C*, *top*). As thymic development proceeds, thymocytes appear to first enter a FcγRII/III$^+$ CD2$^+$ stage (Fig. 2 *C*, *middle*), before the loss of FcγRII/III is accompanied by high expression of CD2 (Fig. 2 *C*, *bottom*). These data suggest the possibility of an early developmental sequence involving the following phenotypic stages of DN thymocytes: FcγRII/III$^+$CD2$^-$ → FcγRII/III$^+$CD2$^+$ → FcγRII/III$^-$ CD2$^+$.

A Fraction of the DN FcγRII/III$^+$ Thymocytes Is Committed to the TCR-γ/δ Lineage. Since the first wave of TCR$^+$ thymocytes in fetal development consists of TCR-γ/δ lineage cells (reviewed in reference 46), the DN FcγRII/III$^+$ thymocyte subset was analyzed for its potential content of TCR-γ/δ lineage cells. Based on the observation that the percentage of TCR-γ/δ lineage cells reaches its peak level (~5% of the total thymocytes) at day 16.5 of gestation (28), fetal thymocytes from this day of gestation were analyzed by flow cytometry for coexpression of FcγRII/III and CD3 (Fig. 3 *C*) or TCR-γ/δ (Fig. 3 *D*), respectively. Negative and single-color controls are shown in Fig. 3, *A* and *B*. Specificity of the anti-CD3 and anti-TCR-γ/δ staining was ensured by control cells that were preincubated with an excess of unlabeled mAb 2C11 (anti-CD3) or unlabeled mAb 3A10 (anti-pan TCR-γ/δ) before staining with 2C11-FITC (Fig. 3, *A* and *B*) or 3A10-FITC (not shown). Confirming the dominance of TCR-γ/δ cells among early TCR thymocytes (28, 46), this analysis revealed ~5% CD3$^+$ cells at day 16.5 of gestation (Fig. 3 *C*) that belong almost entirely to the TCR-γ/δ lineage (Fig. 3 *D*). The vast majority of FcγRII/III$^+$ thymocytes are CD3$^-$, which is consistent with the observed downregulation of FcγRII/III at the DN stage (Fig. 1, *A* and *B*). However, a small fraction of DN FcγRII/III$^+$ thymocytes also coexpress CD3 (Fig. 3 *C*) and are TCR-γ/δ lineage cells (Fig. 3 *D*). 1.4% of the total thymocytes are DN FcγRII/III$^+$ TCR-γ/δ$^+$ thymo-

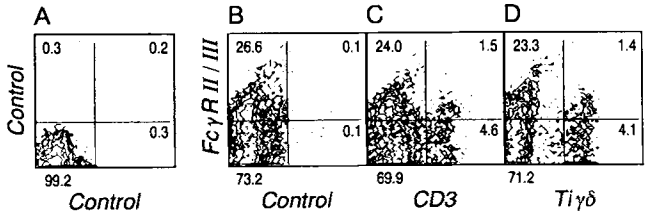

Figure 3. A fraction of DN FcγRII/III$^+$ thymocytes is committed to the TCR-γ/δ lineage. FT day 16.5 were stained with AvPE vs. 2C11-FITC after preincubation with excess of unlabeled 2C11 (*A*), with 2.4G2-biotin followed by AvPE vs. 2C11-FITC after blocking with excess of unlabeled 2C11 (*B*). In *C* and *D*, FT day 16.5 were stained with 2.4G2-biotin followed by AvPE vs. 2C11 (anti-CD3)-FITC (*C*) and 3A10 (anti-pan TCR-γ/δ)-FITC (*D*), respectively.

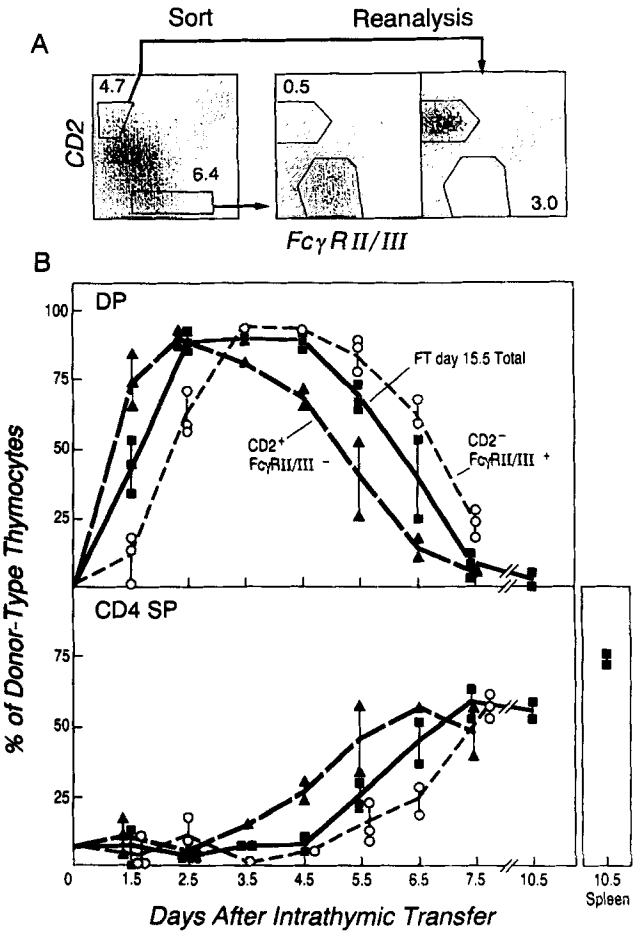

Figure 4. Developmental kinetics in vivo of DN FcγRII/III$^+$CD2$^-$ and DN FcγRII/III$^-$CD2$^+$ delineates early and late stages of DN subsets before differentiation into DP and SP thymocytes. FT day 15.5 derived from timed pregnant C57Bl/6 (Ly5.1) mice were stained for expression of FcγRII/III and CD2, and separated according to the sorting windows shown in *A* (*left*). Reanalysis of sorted FcγRII/III$^+$CD2$^-$ and FcγRII/III$^-$CD2$^+$ subpopulations is shown in *A* (*middle* and *right*, respectively). Subsequently, each subpopulation was injected intrathymically (10^5 cells/thymus) into normal nonirradiated B6Ly5.2 congenic recipient mice. In daily intervals from 1.5 to 7.5 d and on day 10.5 after cell transfer in vivo, donor-type thymocytes were retrieved from recipient thymi and enriched relative to host thymocytes by depletion with anti-Ly-5.2 mAb and goat anti–mouse magnetic beads followed by magnetic separation. Subsequently, developmental progression of donor-type thymocytes was analyzed by three-color immunofluorescence for Ly5.1, CD4, and CD8. Progeny of each subpopulation generate first a single wave of DP (*B*, *top*), and subsequently mature CD4 SP (*B*, *bottom*) and CD8 SP (not shown). Kinetic shifts in this intrathymic development are apparent when comparing total FT day 15.5 (stained for expression of FcγRII/III and CD2 but not separated) (■) with FcγRII/III$^+$CD2$^-$ thymocytes (○) and with FcγRII/III$^-$CD2$^+$ thymocytes (▲), respectively. By day 7.5 and later, the proportion of CD4 SP thymocytes has reached the level found in mature donor-derived peripheral T cells (*B*, *bottom*).

cytes in this experiment. Among the TCR-γ/δ lineage cells this corresponds to ~25% FcγRII/III$^+$. Hence, DN FcγRII/III$^+$ thymocytes contain cells of heterogeneous lineages with the majority apparently being TCR-α/β lineage cell progenitors and a small fraction entering the TCR-γ/δ lineage.

In Vivo Developmental Kinetics of DN FcγRII/III$^+$CD2$^-$ and DN FcγRII/III$^-$CD2$^+$ Thymocytes Delineate Early and Late DN Stages before Differentiation into DP Thymocytes. To test directly the developmental sequence suggested by ex vivo phenotyping of fetal thymocytes for expression of FcγRII/III and CD2, FT day 15.5 were stained for FcγRII/III and CD2 and subsequently separated into FcγRII/III$^+$CD2$^-$ and FcγRII/III$^-$CD2$^+$ subpopulations by cell sorting according to the sorting gates as shown in Fig. 4 *A* (*left*). Day 15.5 of gestation represents a stage of development containing FcγRII/III$^+$CD2$^-$, FcγRII/III$^+$CD2$^+$, and FcγRII/III$^-$CD2$^+$ subpopulations (Fig. 2 *C*, *middle*, and Fig. 4 *A*). Postsorter analysis showed that the isolated FcγRII/III$^+$CD2$^-$ thymocytes contained ≤0.5% of contaminating cells from the FcγRII/III$^-$CD2$^+$ subpopulation. The FcγRII/III$^-$CD2$^+$ subset of DN thymocytes gated by cell sorter was ≤3% contaminated by FcγRII/III$^+$CD2$^-$ thymocytes. Subsequently, the developmental stage and differentiation potential of these early thymocyte subpopulations were assessed. To this end, the in vivo development of total DN day 15.5 thymocytes was compared in parallel to putatively more immature FcγRII/III$^+$CD2$^-$ and more mature FcγRII/III$^-$CD2$^+$ subpopulations, respectively, by intrathymic injection of individual subpopulations.

Since preliminary experiments revealed a general developmental delay of ~4 d when FT day 15.5 were transferred into irradiated recipients when compared with nonirradiated recipients (data not shown), all subsequent experiments for in vivo precursor activity and kinetics were performed in nonirradiated recipients. Precursor cell transfer into the nonirradiated thymic microenvironment should facilitate donor cell development that closely resembles the development in the normal thymus and allows "real-time" measurements between developmental steps in vivo (34). Consequently, cell sorter–purified thymocyte subpopulations from C57Bl/6 mice (Ly5.1) were injected intrathymically (10^5 cells/thymus) into normal, nonirradiated B6Ly5.2 congenic mice. In daily intervals from 1.5 to 7.5 d after cell transfer in vivo, donor-type thymocytes were retrieved from recipient thymi. Donor-type thymocytes were enriched relative to host thymocytes by depletion with anti-Ly5.2 mAb and goat anti-mouse magnetic beads followed by magnetic separation. Subsequently, developmental progression of donor-type thymocytes was analyzed by three-color immunofluorescence for Ly5.1, CD4, and CD8.

All three tested populations from day 15.5 in gestation (FT day 15.5 total, FcγRII/III$^+$CD2$^-$, and FcγRII/III$^-$CD2$^+$) give rise to an initial single wave of DP (Fig. 4 *B*, *top*) and subsequently mature SP thymocytes (Fig. 4 *B*, *bottom*), indicating their T cell progenitor activity in a thymic environment. 2.5 d after intrathymic injection of total FT day 15.5, ~90% of donor-type cells are at the DP stage. Beginning at day 4.5 postinjection (duration of the DP stage ≥48 h), the number of DP declines as donor-type thymocytes are selected into CD4 SP (Fig. 4 *B*) and CD8 SP (not shown) mature cells. By day 7.5 postinjection, <10% of donor-type thymocytes are DP. At this time and later (day 10.5; Fig. 4 *B*, *bottom*), cellular progeny of total day 15.5 fetal progenitors have generated ~60% CD4 SP and ~30% CD8 SP (not shown) thymocytes, thus reflecting the proportions of CD4$^+$ (Fig. 4 *B*, *bottom right*) to CD8$^+$ mature donor-type T cells found in the periphery.

A shift in the kinetics of individual subpopulations was detected when this in vivo differentiation analysis in normal mice was applied in parallel experiments to DN subpopulations characterized by selective expression of FcγRII/III and CD2. Both precursor cell populations give rise to a single wave of DP thymocytes. However, DN FcγRII/III$^+$CD2$^-$ displayed delayed developmental kinetics by ~24 h when compared with total FT day 15.5, while DN FcγRII/III$^-$CD2$^+$ showed accelerated development by ~24 h. To test the statistical significance of the observed kinetic differences, a permutation test was used to analyze the difference between the control population (FT day 15.5 total) and either FcγRII/III$^+$CD2$^-$ (p <0.001) or FcγRII/III$^-$CD2$^+$ (p <0.001). While ~70% of the cellular progeny of DN FcγRII/III$^-$CD2$^+$ were at the DP stage after 1.5 d in vivo, only ~15% of Ly5.1 donor-type cells had developed into DP thymocytes at this time point after injection of DN FcγRII/III$^+$CD2$^-$ (Fig. 4 *B*). Consequently, the first mature SP cells (CD4 SP) began to appear 3.5 d after transfer of DN FcγRII/III$^-$CD2$^+$, in contrast to 5.5 d for DN FcγRII/III$^+$CD2$^-$. Note that the decline of the percent of DP donor-type thymocytes corresponds to the transition from the DP to the SP stage as shown in Fig. 4 *B*. Collectively, these experiments demonstrate that the FcγRII/III$^+$CD2$^-$ subpopulation represents an early DN stage while FcγRII/III$^-$CD2$^+$ mark a late stage among DN fetal thymocytes. The developmental lag time between the two analyzed populations is ~48 h.

TCR β Chain V(D)J Rearrangement Status in FT Day 15.5 Subpopulations. The first molecular hallmark of immature thymocytes entering the Tiα/β lineage is V(D)J rearrangement of the TCR β chain locus followed by VJ rearrangement of the α chain locus (reviewed in reference 9). Thus, V(D)J rearrangement of the TCR β chain locus was analyzed in FcγRII/III$^+$CD2$^-$ and FcγRII/III$^-$CD2$^+$ subpopulations of DN thymocytes derived from day 15.5 of gestation. A sensitive PCR-based analysis for TCR gene rearrangement (36) was used as outlined in Fig. 5 *A*. The PCR amplification was carried out utilizing two sense primers hybridizing to two Vβ genes, Vβ6 and Vβ8, respectively, and one antisense primer recognizing one Jβ element, Jβ2.5. Two different Vβ-specific primers were used to increase the percentage of cells that are included in the analysis for V(D)J rearrangement of the TCR β chain. Since the somatic recombination process leads to joining of a D to a J element and subsequently joining of V to DJ, the DNA sequences that are recognized by the V primers (Vp) and the J primers (Jp) come into proximity after V(D)J rearrangement and allow

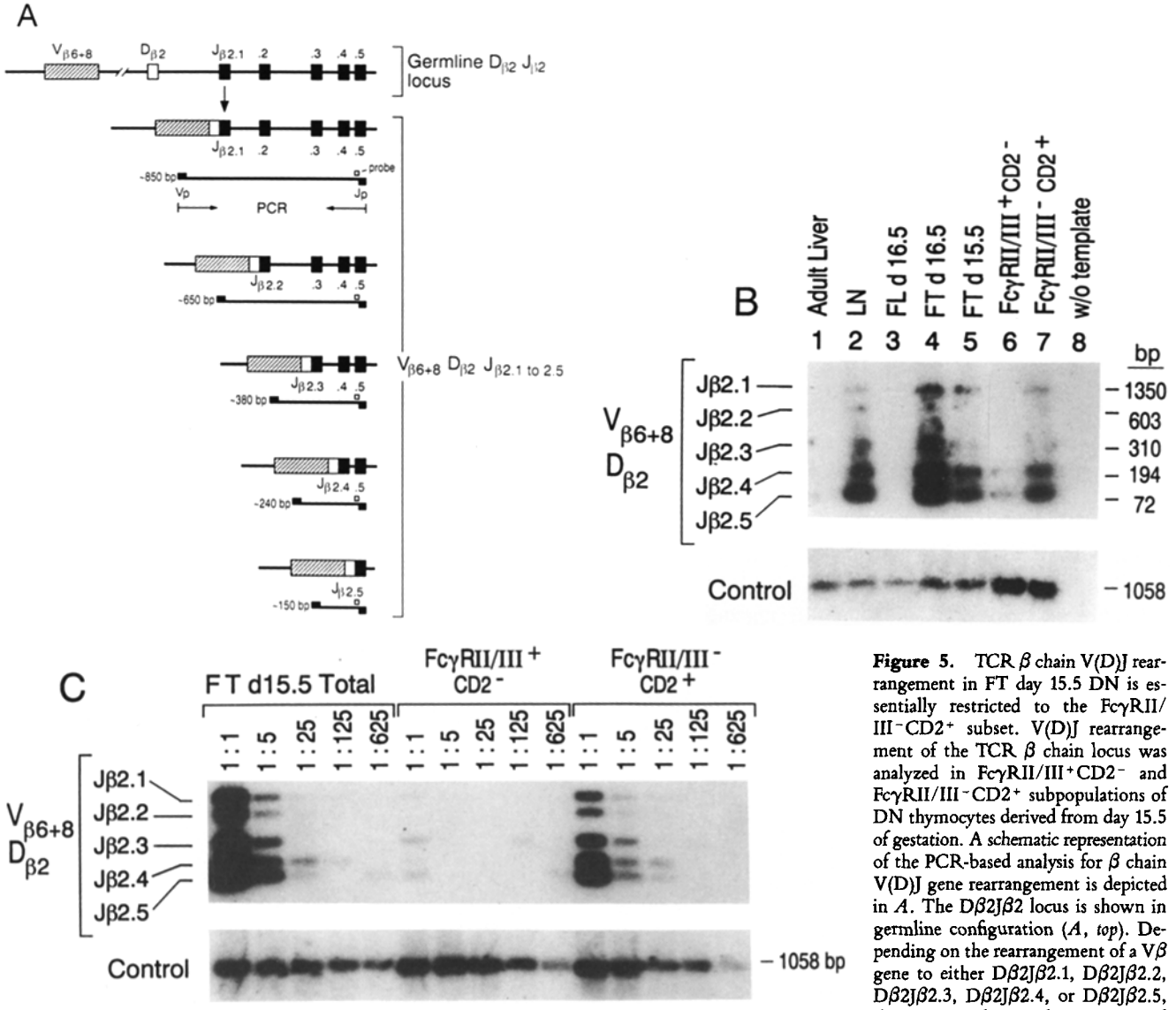

Figure 5. TCR β chain V(D)J rearrangement in FT day 15.5 DN is essentially restricted to the FcγRII/III$^-$CD2$^+$ subset. V(D)J rearrangement of the TCR β chain locus was analyzed in FcγRII/III$^+$CD2$^-$ and FcγRII/III$^-$CD2$^+$ subpopulations of DN thymocytes derived from day 15.5 of gestation. A schematic representation of the PCR-based analysis for β chain V(D)J gene rearrangement is depicted in *A*. The Dβ2Jβ2 locus is shown in germline configuration (*A*, *top*). Depending on the rearrangement of a Vβ gene to either Dβ2Jβ2.1, Dβ2Jβ2.2, Dβ2Jβ2.3, Dβ2Jβ2.4, or Dβ2Jβ2.5, the genomic distance between V and DJ elements will differ (*A*). Five PCR products varying in size from ~850 bp (Vβ6Dβ2Jβ2.1 or Vβ8Dβ2Jβ2.1) to ~150 bp (Vβ6Dβ2Jβ2.5 or Vβ8Dβ2Jβ2.5) are expected (*A*). PCR products were probed by southern hybridization using an oligonucleotide recognizing the 5′ region of the Jβ2.5 element independent from the J primer used for amplification. *B* shows the tissue specificity of TCR β chain V(D)J rearrangement by analyzing genomic DNA derived from adult liver, LN, FL day 16.5, FT day 16.5, and FT day 15.5 (*B*, *top*, lanes *1–5*). In *B*, *bottom*, a control PCR reaction shows a 1,058-bp fragment amplified from exon 8 of CD3ζ (*B*, *bottom*, lanes *1–7*). Omission of template DNA in the reaction mixture gave no PCR products (*B*, lane *8*). In *C*, the relative amounts of V(D)J-rearranged genomic DNA is compared between FT15.5 total (*left*), DN FcγRII/III$^+$CD2$^-$ (*middle*), and DN FcγRII/III$^-$CD2$^+$ (*right*) thymocyte populations. Fivefold titrations of genomic DNA from 1:1 (corresponding to ~100 ng) to 1:625 (~160 pg) were analyzed for V(D)J rearrangements (*C*, *top*) and in parallel for CD3ζ exon 8 as a control (*C*, *bottom*).

PCR amplification. Depending on the Jβ2 element to which either Vβ6 or Vβ8 genes are rearranged, five PCR products are amplified varying in size from ~850 bp (Vβ6Dβ2Jβ2.1 or Vβ8Dβ2Jβ2.1) to ~150 bp (Vβ6Dβ2Jβ2.5 or Vβ8Dβ2Jβ2.5) (see Fig. 5 *A*). To verify the authenticity of the amplified sequences, PCR products were probed by southern hybridization using an oligonucleotide recognizing the 5′ region of the Jβ2.5 element independent from the J primer used for amplification.

To test the tissue specificity of this analysis for TCR β chain rearrangement, genomic DNA was prepared from adult liver, lymph node (LN), fetal liver from day 16.5 in gestation (FL day 16.5), FT day 16.5, and FT day 15.5. As shown in Fig. 5 *B*, V(D)J rearrangement within the β gene locus is clearly detectable in LN, FT 16.5 day, and, to a lesser extent, in FT day 15.5. As expected, no rearrangement is detected in DNA derived from adult liver or FL day 16.5. To demonstrate the presence of intact DNA templates in all samples, a control PCR reaction was performed that amplified a sequence of 1,058 bp within exon 8 of CD3ζ (Fig. 5 *B*, *bottom*),

lanes 1–7) from all templates. Both reactions were template dependent since omission of template DNA in the reaction mixture gave no PCR product (Fig. 5 *B*, lane *8*).

In parallel, V(D)J rearrangement of the β gene locus was compared between the two subpopulations of day 15.5 DN thymocytes that showed kinetic differences in their in vivo development (Fig. 4 *B*). To this end, FcγRII/III$^+$CD2$^-$ and FcγRII/III$^-$CD2$^+$ subpopulations derived from day 15.5 in gestation were separated according to their phenotype by cell sorting (see Fig. 4 *A*), and DNA templates derived from sorted subpopulations were tested for β gene V(D)J rearrangement. Rearrangement was predominantly detected in the FcγRII/III$^-$CD2$^+$ subpopulation as opposed to FcγRII/III$^+$CD2$^-$ thymocytes (Fig. 5 *B*, *top*, lanes *6* and *7*).

Since this first analysis suggested differences in TCR β gene V(D)J rearrangements between DN FcγRII/III$^+$CD2$^-$ and DN FcγRII/III$^-$CD2$^+$ thymocytes, subsequent experiments were performed to quantify such differences. Genomic DNA templates from FT day 15.5 total, DN FcγRII/III$^+$CD2$^-$, and DN FcγRII/III$^-$CD2$^+$ subpopulations were titrated from 1:1 (corresponding to ~100 ng genomic DNA) to 1:625 (~160 pg genomic DNA) and used as templates to detect V(D)Jβ chain rearrangements (Fig. 5 *C*, *top*). Parallel analysis of CD3ζ exon 8 was used as a control (Fig. 5 *C*, *bottom*). Five bands corresponding to Vβ6 + 8Dβ2Jβ2.1–2.5 are clearly detectable using the highest DNA template concentrations in FT day 15.5 total (Fig. 5 *C*, *top left*) and in DN FcγRII/III$^-$CD2$^+$ (Fig. 5 *C*, *top right*). The amount of amplified DNA derived from the highest template concentration (1:1) from DN FcγRII/III$^+$CD2$^-$ thymocytes is comparable to the amount of DNA obtained with the 1:25 template dilution from DN FcγRII/III$^-$CD2$^+$ thymocytes. Two conditions to allow quantification of template DNA by PCR are fulfilled: (*a*) DNA template is not present at saturating amounts since the PCR reaction is sensitive to template titration; and (*b*) the control amplification (Fig. 5 *C*, *bottom*) shows comparable dose-response curves for all three tested populations. If anything, there is more template DNA in the FcγRII/III$^+$CD2$^-$ and FT day 15.5 total samples relative to the FcγRII/III$^-$CD2$^+$ sample based on the control CD3ζ signal. Thus, DN FcγRII/III$^-$CD2$^+$ thymocytes contain ≥25-fold more V(D)J (β chain)-rearranged genomic DNA when compared with DN FcγRII/III$^+$CD2$^-$ thymocytes. Since the sorted populations were ~98% pure, it cannot be excluded that the detectable V(D)J β gene rearrangement among DN FcγRII/III$^+$CD2$^-$ thymocytes is due to contaminating DN FcγRII/III$^-$CD2$^+$ cells. Collectively, these data demonstrate that TCR β gene V(D)J rearrangement at day 15.5 in gestation is predominantly if not exclusively present in the DN FcγRII/III$^-$CD2$^+$ subpopulation, while the majority of the DN FcγRII/III$^+$CD2$^-$ thymocytes represent either cells at a pre-V(D)J (β chain) stage in T cell ontogeny (Fig. 4, *B* and *C*) or separate lineages uncommitted to the TCR-α/β lineage. The latter could include cells of the TCR-γ/δ lineage or non-T cells. However, as shown in Fig. 3, the γ/δ population represents a minor fraction of fetal DN FcγRII/III$^+$ thymocytes. Furthermore, the high level of Thy-1 expression is consistent with a T lineage designation of the majority of FcγRII/III$^+$CD2$^-$ thymocytes.

The Majority of Adult Thymocytes from Rearrangement-deficient RAG-2$^{-/-}$ Mice Are Developmentally Arrested at the DN CD2$^-$ Stage. Since the expression of FcγRII/III marks an early pre-Vβ(Dβ)Jβ rearrangement stage in immature thymocytes and the majority of DN FcγRII/III$^-$CD2$^+$ thymocytes represent a V(D)J-rearranged stage, we next analyzed adult thymocytes from recombination-activating gene 2 (RAG-2)-deficient mice (19) for expression of FcγRII/III and CD2. B and T cells from RAG-2$^{-/-}$ mice are unable to rearrange their Ig and TCR genes, respectively, and RAG-2$^{-/-}$ thymocytes have previously been shown to be developmentally arrested at the DN stage (19). Normal adult mouse thymocytes (see below) as well as thymocytes derived from adult RAG-2$^{+/-}$ mice contain <3% of FcγRII/III-expressing cells (Fig. 6 *A–C*, *top*). In contrast, ~15% of thymocytes derived from RAG-2$^{-/-}$ mice are FcγRII/III$^+$ (Fig. 6, *A–C*, *bottom*), showing that FcγRII/III$^+$ expression is not blocked by the RAG-2 defect. To further analyze this thymocyte subset phenotypically, thymocytes derived from RAG-2$^{+/-}$ mice and RAG-2$^{-/-}$ mice were analyzed by two-color immunofluorescence for expression of FcγRII/III vs. Thy-1, HSA, and CD2, respectively. To exclude the possibility that the hypocellular thymus from RAG-2$^{-/-}$ mice (~100-fold reduction in the total cell number of thymocytes [19]) contains relatively enriched populations of contaminating FcγRII/III$^+$ macrophages or granulocytes, thymocytes from RAG-2$^{+/-}$ mice and RAG-2$^{-/-}$ mice were analyzed for coexpression of Thy-1 and HSA vs. FcγRII/III. As shown in Fig. 6, *A* and *B*, while a small fraction of the FcγRII/III$^+$ thymocytes was Thy-1$^-$ and HSA$^-$, the majority coexpressed high levels of Thy-1 (Fig. 6 *A*, *bottom*) and HSA (Fig. 6 *B*, *bottom*), which are phenotypic characteristics of immature thymocytes.

In view of the fact that the in vivo kinetic experiments using fetal thymocytes had indicated a maturation sequence of FcγRII/III$^+$CD2$^-$ → FcγRII/III$^+$CD2$^+$ → FcγRII/III$^-$CD2$^+$, we next analyzed thymocytes from adult RAG-2$^{+/-}$ mice and RAG-2$^{-/-}$ mice for expression of FcγRII/III and CD2 (Fig. 6 *C*). Interestingly, this phenotypic comparison revealed that the development of DN thymocytes in RAG-2$^{-/-}$ mice is blocked before the FcγRII/III$^-$CD2$^+$ stage. While RAG-2$^{+/-}$ mice as well as normal adult mice contain ~95% FcγRII/III$^-$CD2$^+$ thymocytes and <3% FcγRII/III$^+$CD2$^+$ cells (Fig. 6 *C*, *top*), <3% of RAG-2$^{-/-}$ thymocytes are FcγRII/III$^-$CD2$^+$ (Fig. 6 *C*, *bottom*). In contrast to the virtually complete absence of CD4 and CD8 expression in RAG-2$^{-/-}$ thymocytes, however, CD2 expression is not completely abrogated in RAG-2$^{-/-}$ mice. Nevertheless, CD2 expression is restricted to <10% of thymocytes and is largely confined to the FcγRII/III$^+$CD2$^+$ subset. However, the majority (~70%) of FcγRII/III$^+$ thymocytes is CD2$^-$. It thus appears that two stages of early thymocyte development (DN FcγRII/III$^+$CD2$^-$ and DN FcγRII/III$^+$CD2$^+$) that were detect-

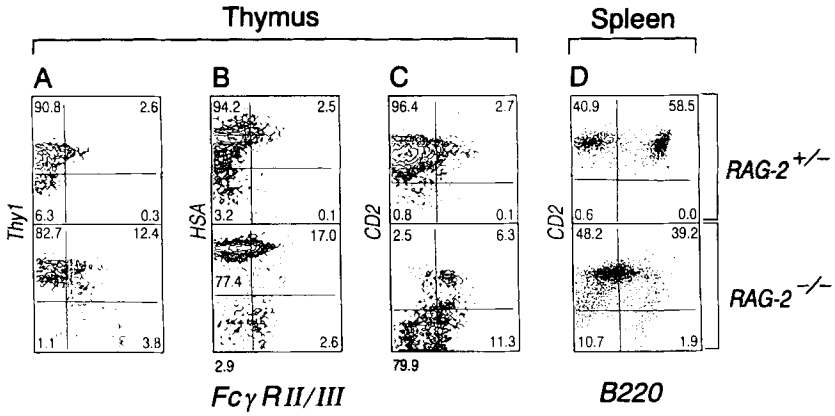

Figure 6. Phenotypic analysis of adult thymocytes from rearrangement-deficient RAG-2$^{-/-}$ mice reveals a developmental arrest at the DN CD2$^-$ stage. Thymocytes (*A–C*) and splenocytes (*D*) were derived from 6-wk-old homozygous RAG-2$^{-/-}$-deficient mice (*bottom*) and from heterozygous control animals (RAG-2$^{+/-}$) (*top*). Thymocytes were analyzed for expression of FcγRII/III vs. Thy-1 (*A*), HSA (*B*), and CD2 (*C*). Splenocytes were analyzed for expression of CD2 vs. B220 (*D*). RAG-2$^{+/-}$ thymocytes contain <3% of FcγRII/III-expressing cells (*top*), while ~15% of thymocytes derived from RAG-2$^{-/-}$ mice are FcγRII/III$^+$ (*bottom*). Note the dramatic reduction in the percentage of FcγRII/III$^-$CD2$^+$ in RAG-2$^{-/-}$ thymocytes (*C*, *bottom*) when compared with RAG-2$^{+/-}$ thymocytes (*C*, *top*).

able in fetal mice are present and, on a percentage basis, overrepresented in RAG-2$^{-/-}$ mice due to the developmental arrest. Thus, the developmental progression of thymocytes entering the TCR-α/β pathway as observed in fetal mice (Fig. 2 *C*) appears to be blocked immediately before entry into the FcγRII/III$^-$CD2$^+$ stage in thymocytes due to the RAG-2 mutation, which prevents TCR gene rearrangement. However, ~80% of the adult RAG-2$^{-/-}$ thymocytes express neither CD2 nor FcγRII/III and thus cannot be assigned to the developmental sequence described herein. Note that in view of the hypocellularity of the RAG-2$^{-/-}$ thymus (19), the absolute number of FcγRII/III$^+$ thymocytes is not increased, suggesting that the rearrangement defect perturbs early development, which directly or indirectly affects the generation of FcγRII/III$^+$ and CD2$^+$ thymocytes.

In contrast to mature human B lymphocytes, murine B cells express CD2 (47, 48). The finding that the expression of CD2 in thymocytes is largely abrogated in RAG-2$^{-/-}$ mice (Fig. 6 *C*) prompted us to analyze the potential influence of the developmental blockade at the pro-B cell stage (Ig genes in germline, B220^{low}) on the expression of CD2 in RAG-2$^{-/-}$ mice. Splenocytes derived from RAG-2$^{+/-}$ (Fig. 6 *D*, *top*) and RAG-2$^{-/-}$ (Fig. 6 *D*, *bottom*) mice were analyzed for expression of CD2 vs. B220. While the majority of B lineage cells in the RAG-2$^{+/-}$ spleen express high levels of B220, B lineage cells from RAG-2$^{-/-}$ mice express low levels of B220 (Fig. 6 *D*, *bottom*), as described (19, 49). All B220^{high} splenocytes from RAG-2$^{+/-}$ spleen coexpress CD2. In contrast, RAG-2$^{-/-}$ splenocytes contain both B220$^+$CD2$^+$ and B220$^+$CD2$^-$ cells, suggesting that CD2 can be expressed in B cell progenitors that carry their Ig genes still in germline configuration. Thus, in contrast to T cell progenitors, the RAG-2 mutation does not appear to block CD2 expression in the B lineage.

Normal Adult CD3$^-$CD4$^-$CD8$^-$ Thymocytes Contain FcγRII/III$^+$CD2$^-$, FcγRII/III$^+$CD2$^+$ and FcγRII/III$^-$CD2$^+$ Subpopulations. To test whether FcγRII/III$^+$CD2$^-$, FcγRII/III$^+$CD2$^+$, or FcγRII/III$^-$CD2$^+$ thymocyte subpopulations are also present in postnatal life among immature thymocytes, CD3$^-$CD4$^-$CD8$^-$ thymocytes were purified from the adult thymus. To this end, adult thymocytes were stained with a combination of anti-CD3, anti-CD4, and anti-CD8 mAbs, and antibody-coated cells were subsequently removed by two rounds of magnetic bead depletion followed by cell sorter separation. This purification method yielded ~98% pure CD3$^-$CD4$^-$CD8$^-$ thymocytes. CD3$^-$CD4$^-$CD8$^-$ thymocytes were then examined for expression of FcγRII/III and CD2 (Fig. 7 *D*). Negative controls as well as single-color controls are shown in Fig. 7, *A–C*. To test specific binding of mAb 2.4G2 to the thymocytes, the binding of 2.4G2-FITC was blocked by preincubation with excess of unlabeled 2.4G2 (Fig. 7 *A*). ~15% of CD3$^-$CD4$^-$CD8$^-$ thymocytes express FcγRII/III (Fig. 7 *B*), and ~20% stain weakly for CD2 (Fig. 7 *C*). Two-color FcγRII/III and CD2 fluorescence analysis reveals ~12% FcγRII/III$^+$CD2$^-$, ~4% FcγRII/III$^+$CD2$^+$, and ~16% FcγRII/III$^-$CD2$^+$ thymocytes (Fig. 7 *D*). These subpopulations of FcγRII/III$^+$CD2$^-$ and FcγRII/III$^-$CD2$^+$ among normal adult CD3$^-$CD4$^-$CD8$^-$ thymocytes resemble the phenotypic subpopulations identified in fetal development (Fig. 2 *C*), as well as after the developmental arrest in RAG-2-deficient mice (Fig. 7 *C*). In contrast to RAG-2$^{-/-}$ thymocytes, however, normal adult CD3$^-$ CD4$^-$CD8$^-$ thymocytes do contain a substantial percentage of FcγRII/III$^-$CD2$^+$ cells (>15%).

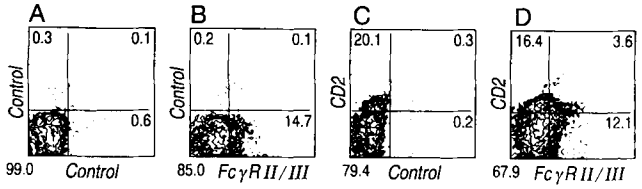

Figure 7. Phenotypic analysis of adult CD3$^-$CD4$^-$CD8$^-$ thymocytes identifies FcγRII/III$^+$CD2$^-$, FcγRII/III$^+$CD2$^+$, and FcγRII/III$^+$ CD2$^+$ subpopulations in postnatal life. Adult CD3$^-$CD4$^-$CD8$^-$ thymocytes are prepared as described in Materials and Methods. Cells were stained with avidin-PE vs. 2.4G2-FITC after preincubation with excess of unlabeled 2.4G2 (*A*), for avidin-PE vs. 2.4G2-FITC (*B*), for CD2-biotin followed by avidin-PE vs. 2.4G2-FITC after preincubation with excess of unlabeled 2.4G2 (*C*) and with CD2-biotin followed by avidin-PE vs. 2.4G2-FITC (*D*).

Discussion

In previous work, we have identified the expression of Fcγ receptors for IgG (FcγRII/III, CD16) on the majority of early fetal (DN) thymocytes (13). In addition to the early appearance of this cell population in thymic ontogeny, several observations suggested that the FcγRII/III$^+$ thymocyte population would represent an early stage in T cell development. First, this cell population contains relatively uncommitted cells, which could give rise to T cells and NK cells in a microenvironment-dependent way. Second, FcγRII/III expression was shown to be downregulated early in thymocyte development (between the DN and DP stages). Although FcγRII/III expression precedes the cell surface expression of TCR-α/β by several days in gestation, FcγRII/III downregulation appears to correlate with the entry of developing thymocytes into the TCR Tiα/β lineage pathway. Support for this view comes from the finding that loss of FcγRII/III expression is only induced in the thymus. In contrast, early fetal thymocytes grown in in vitro suspension cultures in the presence of IL-2, or "parked" in the spleen in vivo after intravenous transfer of donor-type fetal thymocytes, maintained expression of FcγRII/III (13).

Here we provide further evidence that FcγRII/III expression is detectable at very early stages of intrathymic development and, more precisely, characterized its appearance and disappearance. We observe that on day 15.5 of gestation, the majority of the ontogenetically primitive population of CD4^{low} SP thymocytes is FcγRII/III$^+$ (Fig. 1 *D*). Moreover, fractions of FcγRII/III$^+$ thymocytes include Thy-1^{low}, IL-2R (p55)$^-$, CD2$^-$, and HSA^{low} cells (Fig. 2, *A–D*). Very early intrathymic progenitor populations have been phenotypically characterized as Thy-1^{low}, Sca1$^+$, HSA^{low}, Pgp-1$^+$, CD3$^-$, CD4$^{-/low}$, CD8$^-$, IL-2R (p55)$^-$ (38, 42, 43, 45, 50). Consequently, the phenotype of at least a fraction of the FcγRII/III-expressing thymocytes is consistent with the expression pattern of very early thymocytes. However, FcγRII/III-expressing thymocytes also include more mature DN stages of thymocyte development.

In preliminary experiments designed to test whether prethymic hematopoietic cells derived from fetal liver contain FcγRII/III$^+$ T cell progenitors, we isolated FcγRII/III$^+$ fetal liver cells from day 15.5 in gestation (representing 5–15% of the total population), and analyzed their developmental potential upon intrathymic injection in vivo. FcγRII/III$^+$ fetal liver cells contained T cell progenitor activity, but did not appear to provide a means to enrich for such activity since FcγRII/III$^-$ fetal liver cells also expressed T cell progenitor activity (not shown). Collectively, these experiments indicate that developing thymocytes express FcγRII/III very early in T cell ontogeny and that fetal liver–derived T cell progenitors potentially carry FcγRII/III as thymic immigrants.

The progenitor activity of DN FcγRII/III$^+$ cells for the generation of TCR-α/β^+ thymocytes inside the thymus has been demonstrated (13). In the present work, the kinetics of this in vivo differentiation is described in detail. It is also likely that a fraction of DN FcγRII/III$^-$ thymocytes enters the TCR-γ/δ lineage. While we have previously identified FcγRII/III$^+$ TCR-γ/δ^+ thymocytes after in vitro culture of fetal thymocytes in the presence of IL-2 (13), the current study demonstrates the presence of such cells in situ. Although the precursor-product relationship of DN FcγRII/III$^+$ thymocytes and mature TCR-γ/δ^+ T cells remains to be directly shown, it is conceivable that the FcγRII/III$^+$ TCR-γ/δ^+ thymocytes identified herein represent an intrathymic stage of TCR-γ/δ epidermal dendritic T cells. It is noteworthy that these epidermal cells express FcγRII/III (51).

Developing thymocytes entering the TCR-α/β pathway cease to express FcγRII/III at the DN stage and before the entry into the CD3$^-$CD8^{low} stage. Later phases of thymocytes (DP and mature SP) are FcγRII/III$^-$ (Fig. 1 *B*). This downregulation of FcγRII/III expression at an immature thymocyte stage is in contrast to FcγRII expression during B cell ontogeny. Recently, phenotypic analysis of developing B cells has demonstrated the expression of FcγRII as early as at the pre-B cell stage (52). Unlike mature T cells, however, B lineage cells continue to express Fcγ receptors as mature B cells (53, 54).

Interestingly, the downregulation of FcγRII/III expression on DN thymocytes entering the TCR-α/β pathway contrasts with the upregulation of CD2 just before the exit from the DN stage and allows the separation of DN thymocytes into three novel phenotypic subsets. The sequential appearance in thymic ontogeny of first FcγRII/III$^+$CD2$^-$ and latter FcγRII/III$^-$CD2$^+$ thymocytes (Fig. 2 *C*) was assessed by flow cytometry. Moreover, the developmental delay of CD4 and CD8 coexpression as well as the generation of mature SP thymocytes (Fig. 4 *B*) by ~48 h after intrathymic injection of FcγRII/III$^+$CD2$^-$ when compared with FcγRII/III$^-$CD2$^+$ characterize FcγRII/III$^+$CD2$^-$ and FcγRII/III$^-$CD2$^+$ DN subsets as distinct early and late stages, respectively, of the same pathway leading into the Tiα/β lineage.

Our kinetic measurements of the development of fetal thymocytes entering the TCR-α/β pathway after adoptive transfer into normal nonirradiated recipients are consistent with previously reported in vivo kinetics of developing thymocytes. The transition time from the DN to the DP stage, ranging from 1.5 d (FcγRII/III$^+$CD2$^-$) to 3.5 d (FcγRII/III$^-$CD2$^+$) (Fig. 4 *B*), resembles the in vivo kinetics reported by Petri et al. (34), who compared maturational stages of adult DN Pgp-1$^-$ IL-2Rα^+ and DN Pgp-1$^-$ IL-2Rα^- thymocytes in normal recipient mice. Progeny of FcγRII/III$^+$CD2$^-$ and FcγRII/III$^-$CD2$^+$ DN thymocytes remain at the DP stage for 48–72 h (Fig. 4 *B*) before they are selected into the SP thymocyte compartment (Fig. 4 *C*). Huesmann et al. (55) estimated the life span of DP thymocytes in TCR transgenic mice using bromodeoxyuridine (BrdU) labeling in vivo to be 3.5 d. Thus, both in vivo DNA labeling and adoptive transfer of precursor populations into normal, nonirradiated recipients yield comparable kinetics and are most likely to reflect the steady-state physiology of intrathymic T cell development.

Undifferentiated "prothymocytes" entering the thymus

carry their TCR genes in germline configuration (38, 43). Subsequently, these precursors may evolve along TCR-γ/δ, TCR-α/β, or non-T lineages. The order of somatic recombination events acting on the different TCR gene loci in thymocytes at the early stages of thymocyte differentiation is developmentally regulated (7, 8). The somatic recombination process in Tiα/β T cell progenitors leading to antigen receptor diversity in mature lymphocytes begins by rearrangement of first the TCR β locus (β chain V[D]J joining first detectable at day 15 in gestation) and subsequently the TCR α locus. Transcripts encoding both TCR chains are expressed by day 17 in gestation (reviewed in reference 9). Our analysis of the V(D)J β gene rearrangement status in DN subpopulations at day 15.5 in gestation has identified DN FcγRII/III$^+$ CD2$^-$ cells as being primarily at a pre-V(D)J stage, whereas V(D)J β chain rearrangement is readily apparent in the FcγRII/III$^-$CD2$^+$ subset. Although some DN FcγRII/III$^+$CD2$^-$ cells may be committed to the TCR-γ/δ rather than TCR-α/β lineage, this fraction is small (Fig. 3). Likewise, the pool of non-T lineage cells contained within the DN FcγRII/III$^+$CD2$^-$ subpopulation appears small given the high Thy-1 and HSA expression on this population (Fig. 2). The difference in rearrangement status directly supports our suggestion that DN FcγRII/III$^+$CD2$^-$ and DN FcγRII/III$^-$CD2$^+$ cells are early and late DN populations, respectively. Furthermore, V(D)J β chain rearrangement is temporally correlated with the termination of FcγRII/III expression.

The molecular understanding of antigen receptor gene rearrangement has been advanced by the identification of two recombination activation genes, termed RAG-1 and RAG-2 (reviewed in references 56 and 57). RAG-1 and RAG-2 mRNAs are expressed in immature B and T lymphocyte progenitor populations that actively rearrange their antigen receptor genes. Together, these genes confer recombination activity upon transfection into nonrearranging cells (18). Until recently, little was known about the influence of productive TCR gene rearrangements on the regulation of intrathymic developmental progression. Gene-targeting experiments in which RAG-1 or RAG-2 loci were mutated have now demonstrated the essential nature of both genes for the somatic recombination process (19, 49). Mice expressing the RAG-1$^{-/-}$ or RAG-2$^{-/-}$ genotype lack both mature B and T lymphocytes and thus, in phenotype, resemble animals with a naturally occurring SCID syndrome (reviewed in reference 58). Specifically, thymocytes from RAG-2$^{-/-}$ mice are developmentally arrested at the DN stage before the assembly and surface expression of the TCR. In addition, the RAG-2 mutation leads to a reduction to ~1% of the normal number of thymocytes (19). Similar effects have been noted in SCID mice since SCID thymocytes are also arrested at the DN stage (58).

While both DN FcγRII/III$^+$CD2$^-$ and DN FcγRII/III$^+$CD2$^+$ populations are present and their relative percentages enriched in RAG-2$^{-/-}$ when compared with RAG-2$^{+/-}$ thymocytes, strikingly, the DN FcγRII/III$^-$CD2$^+$ population is reduced from >95% (RAG-2$^{+/-}$) to <3% (RAG-2$^{-/-}$) (Fig. 6 *C*). Thus, persistence of TCR genes in germline configuration in the early developing thymocytes has a dramatic inhibitory effect, directly or indirectly, on CD2 expression at the late DN stage. Expression of CD2 occurs after V(D)J β chain rearrangement in thymic development and, much like CD4 and CD8 expression (19, 49), appears to be, in large part, linked to V(D)J β chain rearrangement. In this context, it is interesting that transfection of a TCR β chain gene into a SCID-derived cell line led to upregulation of CD2 surface expression in addition to surface expression of a Ti β-β homodimer (59). The mechanism by which the rearranged TCR β chain mediates transcriptional and/or translational control of these genes and their products remains to be determined. These results suggest that the expression of the TCR β chain provides a critical signal for development beyond the DN and into the DP stage. Consistent with this hypothesis, SCID mice expressing a transgenic TCR β chain contain normal percentages of DP thymocytes (59). Moreover, in RAG-1$^{-/-}$ and RAG-2$^{-/-}$ mice, which carry fully rearranged transgenic TCR β chains, thymocytes are released from their differentiation block at the DN stage and progress into the DP stage (60, 61).

The role of FcγRII/III on early CD4^{low} thymocytes and DN thymocytes during thymic differentiation is unknown. However, signaling function through the associated FcϵRIγ (62) or CD3ζ (63–65) subunits may be important in the developmental process. mRNAs encoding FcϵRIγ and CD3ζ proteins are present in the developing thymus as early as day 14 of gestation (13; data not shown). While IgG is the ligand of FcγRII/III on mature hematopoietic elements and NK cells, it is possible that an alternative ligand interacts with the ectodomain of FcγRII/III expressed on early thymic precursors. It is now important to define the precise function of this molecule during thymocyte development.

It is apparent that there is no requirement for CD2 expression before induction of TCR gene rearrangement. This notion is consistent with the previous demonstration of the presence of CD2$^-$CD3$^+$ DN thymocytes in the mouse (14). Rather, TCR β gene V(D)J rearrangement in DN thymocytes is necessary for normal CD2 surface expression. More specifically, fixation of the TCR genes in germline configuration largely prevents the differentiation of DN thymocytes into the FcγRII/III$^-$CD2$^+$ stage. It is undoubtedly noteworthy that CD2 expression precedes and is maintained through the DP thymocyte stage because it is at this latter stage that positive and negative selection events are ongoing. The adhesion function of CD2 may well facilitate cell-cell contact important in the thymic "education" process. In this regard, repertoire selection of the TCRs in humans and mice could be influenced by the presence of CD2. Clearly, further studies are required to address this issue, particularly because murine and human CD2 bind related but distinct ligands, CD48 and CD58 (LFA-3), respectively, with different tissue distributions (66). Nonetheless, the functional dissection provided by the elucidation of the DN subpopulations described through our analysis should allow us to further define the orderly steps in thymic development in the mouse.

We thank Dr. S. Kimura (Memorial Sloan-Kettering Institute, New York) for his gifts of mAbs; Dr. C. Reeder (National Cancer Institute, Frederick, MD) for congenic mice; Ms. M. Mann and the Redstone Animal Facility staff (Dana-Farber Cancer Institute) for their care in maintenance of mouse colonies; P. Lopez, M. Demaria, and M. Handley for cell sorter expertise; Dr. L. Clayton (DFCI) for CD3ζ-specific oligonucleotides; and Dr. A. Kruisbeek (Netherlands Cancer Institute, Amsterdam) for critically reading the manuscript.

This work was supported in part by National Institutes of Health grants AI-21226 and AI-19807 to E. L. Reinherz, and AI-20047 to F. W. Alt.

Address correspondence to H.-R. Rodewald, Laboratory of Immunobiology, Dana-Farber Cancer Institute, 44 Binney Street, Boston, MA 02115. H.-R. Rodewald's present address is the Basel Institute for Immunology, Grenzacherstrasse 487, CH-4005 Basel, Switzerland.

Received for publication 22 October 1992 and in revised form 28 December 1992.

References

1. Owen, J.J.T., and M.A. Ritter. 1969. Tissue interaction in the development of thymus lymphocytes. *J. Exp. Med.* 129:431.
2. Fontaine-Perus, J.C., F.M. Calman, C. Kaplan, and N.M. Le Douarin. 1981. Seeding of the 10-day mouse embryo thymic rudiment by lymphocyte precursors in vitro. *J. Immunol.* 126:2310.
3. Adkins, B., C. Mueller, C.Y. Okada, R.A. Reichert, J.L. Weissman, and G.J. Spangrude. 1987. Early events in T cell maturation. *Annu. Rev. Immunol.* 5:325.
4. Scollay, R., A. Wilson, A. D'Amico, R. Kelly, M. Egerton, M. Pearse, L. Wu, and K. Shortman. 1988. Developmental status and reconstitution potential of subpopulations of murine thymocytes. *Immunol. Rev.* 104:81.
5. Fowlkes, B.J., and D.M. Pardoll. 1989. Molecular and cellular events of T cell development. *Adv. Immunol.* 44:207.
6. Nikolic-Zugic, J. 1991. Phenotypic and functional stages in the intrathymic development of αβ T cells. *Immunol. Today.* 12:65.
7. Raulet, D.H., R.D. Garman, H. Saito, and S. Tonegawa. 1985. Developmental regulation of T-cell receptor gene expression. *Nature (Lond.).* 314:103.
8. Snodgrass, H.R., Z. Dembic, M. Steinmetz, and H. v. Boehmer. 1985. Expression of T-cell antigen receptor genes during fetal development in the thymus. *Nature (Lond.).* 315:232.
9. Kronenberg, M., G. Siu, L.E. Hood, and N. Shastri. 1986. The molecular genetics of the T cell antigen receptor and T cell antigen recognition. *Annu. Rev. Immunol.* 4:529.
10. Nikolic-Zugic, J., and M.J. Bevan. 1988. Thymocytes expressing CD8 differentiate into $CD4^+$ cells following intrathymic injection. *Proc. Natl. Acad. Sci. USA.* 85:8633.
11. Guidos, G.J., I.L. Weissman, and B. Adkins. 1989. Intrathymic maturation of murine T lymphocytes from $CD8^+$ precursors. *Proc. Natl. Acad. Sci. USA.* 86:7542.
12. von Boehmer, H. 1990. Developmental biology of T cells in T cell receptor transgenic mice. *Annu. Rev. Immunol.* 8:531.
13. Rodewald, H.-R., P. Moingeon, J.L. Lucich, C. Dosiou, P. Lopez, and E.L. Reinherz. 1992. A population of early fetal thymocytes expressing FcγRII/III contains precursors of T lymphocytes and NK cells. *Cell.* 69:139.
14. Yagita, H., J. Asakawa, S. Tansyo, T. Nakamura, S. Habu, and K. Okumura. 1989. Expression and function of CD2 during murine thymocyte ontogeny. *Eur. J. Immunol.* 19:2211.
15. Sen, J., R.J. Arceci, W. Jones, and S.J. Burakoff. 1989. Expression and ontogeny of murine CD2. *Eur. J. Immunol.* 19:1297.
16. Reinherz, E.L. 1985. A molecular basis for thymic selection: regulation of T11 induced thymocyte expansion by the T3-Ti antigen/MHC receptor pathway. *Immunol. Today.* 6:75.
17. Schatz, D.G., M.A. Oettinger, and D. Baltimore. 1989. The V(D)J recombination activating gene, RAG-1. *Cell.* 59:1035.
18. Oettinger, M.A., D.G. Schatz, C. Gorka, and D. Baltimore. 1990. RAG-1 and RAG-2, adjacent genes that synergistically activate V(D)J recombination. *Science (Wash. DC).* 248:1517.
19. Shinkai, Y., G. Rathbun, K.-P. Lam, E.M. Oltz, V. Stewart, M. Mendelsohn, J. Charron, M. Datta, F. Young, A.M. Stall, and F.W. Alt. 1992. RAG-2 deficient mice lack mature lymphocytes owing to inability to initiate V(D)J rearrangements. *Cell.* 68:855.
20. Unkeless, J.C. 1979. Characterization of a monoclonal antibody directed against mouse macrophage and lymphocyte Fc receptors. *J. Exp. Med.* 150:580.
21. Ledbetter, J.A., and L.A. Herzenberg. 1979. Xenogeneic monoclonal antibodies to mouse lymphoid differentiation antigens. *Immunol. Rev.* 47:63.
22. Bruce, J., F.W. Symington, T.J. McKearn, and J. Sprent. 1981. A monoclonal antibody discriminating between subsets of T and B cells. *J. Immunol.* 127:2496.
23. Malek, T.R., R.J. Robb, and E.M. Shevach. 1983. Identification and initial characterization of a rat monoclonal antibody reactive with the murine interleukin 2 receptor-ligand complex. *Proc. Natl. Acad. Sci. USA.* 80:5694.
24. Yagita, H., T. Nakamura, H. Karasuyama, and K. Okumura. 1989. Monoclonal antibodies specific for murine CD2 reveal its presence on B as well as T cells. *Proc. Natl. Acad. Sci. USA.* 86:645.
25. Furth, M.E., L.J. Davis, B. Fleurdelys, and E.M. Scolnick. 1982. Monoclonal antibodies to the p21 products of the transforming gene of Harvey Murine Sarcoma virus and of the cellular ras gene family. *J. Virol.* 43:294.
26. Portoles, P., J. Rojo, A. Golby, M. Bonneville, S. Gromkowski, L. Greenbaum, C. Janeway, D. Murphy, and K. Bottomly. 1989. Monoclonal antibodies to murine CD3ε define distinct epitopes, one of which may interact with CD4 during T cell activation. *J. Immunol.* 142:4269.
27. Leo, O., M. Foo, D.H. Sachs, L.E. Samelson, and J.A. Bluestone. 1987. Identification of a monoclonal antibody specific for a murine T3 polypeptide. *Proc. Natl. Acad. Sci. USA.* 84:1374.
28. Itohara, S., N. Nakanishi, O. Kanagawa, R. Kubo, and S. Tonegawa. 1989. Monoclonal antibodies specific to native mu-

rine T cell receptor γδ: analysis of γδ T cells during thymic ontogeny and in peripheral lymphoid organs. *Proc. Natl. Acad. Sci. USA.* 86:5094.
29. Dialynas, D.P., D.B. Wilde, P. Marrack, A. Pierres, K.A. Wall, W. Havran, G. Otten, M.R. Loken, M. Pierres, J. Kappler, and F.W. Fitch. 1983. Characterization of the murine antigenic determinant, designated L3T4a, recognized by monoclonal antibody GK1.5: expression of L3T4a by functional T cell clones appears to correlate primarily with class II MHC antigen reactivity. *Immunol. Rev.* 74:29.
30. Coffman, R.L., and I.L. Weissman. 1981. B220: a B cell specific member of the T 200 glycoprotein family. *Nature (Lond.).* 289:681.
31. Shen, F.-W. 1981. Monoclonal antibodies to mouse lymphocyte differentiation alloantigens. *In* Monoclonal Antibodies and T Cell Hybridomas. G. Haemmerling, U. Haemmerling, and J.F. Kearney, editors. Elsevier Science Publishers B.V., Amsterdam. 25–31.
32. Johnson, G.D., and E.J. Holborow. 1986. Preparation and use of fluorochrome conjugates. *In* Handbook of Experimental Immunology, vol. I. D. Weir, editor. Oxford University Press, Oxford. 28.1–28.21.
33. Goldschneider, I., K.L. Komschlies, and D.L. Greiner. 1986. Studies of thymocytopoiesis in rats and mice. I. Kinetics of appearance of thymocytes using a direct intrathymic adoptive transfer assay for thymocyte precursors. *J. Exp. Med.* 163:1.
34. Petrie, H.T., P. Hugo, R. Scollay, and K. Shortman. 1990. Lineage relationships and developmental kinetics of immature thymocytes: CD3, CD4, and CD8 acquisition in vivo and in vitro. *J. Exp. Med.* 172:1583.
35. Hogan, B., F. Constantini, and E. Lacy. 1986. Manipulating the Mouse Embryo: A Laboratory Manual. Cold Spring Harbor Laboratory, Cold Spring Harbor, NY.
36. D'Adamio, L., L.K. Clayton, K.M. Awad, and E.L. Reinherz. 1992. Negative selection of thymocytes: a novel polymerase chain reaction-based molecular analysis detects requirements for macromolecular synthesis. *J. Immunol.* 149:3550.
37. Cox, D.R., and A.V. Hinkley. 1974. Theoretical Statistics. Chapman and Hall Ltd., London, 179 pp.
38. Wu, L., R. Scollay, M. Egerton, M. Pearse, G.J. Spangrude, and K. Shortman. 1991. CD4 expressed on earliest T lineage precursor cells in the adult murine thymus. *Nature (Lond.).* 349:71.
39. Wu, L., M. Antica, G.R. Johnson, R. Scollay, and K. Shortman. 1991. Developmental potential of the earliest precursor cells from the adult mouse thymus. *J. Exp. Med.* 174:1617.
40. Howe, R.C., and H.R. MacDonald. 1988. Heterogeneity of immature ($Lyt2^-/L3T4^-$) thymocytes: identification of four major phenotypically distinct subsets differing in cell cycle status and in vitro activation requirements. *J. Immunol.* 140:1047.
41. Wilson, A., A. D'Amico, T. Ewing, R. Scollay, and K. Shortman. 1988. Subpopulations of early thymocytes: a cross-correlation flow cytometric analysis of adult mouse $Lyt2^-L3T4^-$ ($CD8^-CD4^-$) thymocytes using eight different surface markers. *J. Immunol.* 140:1461.
42. Pearse, M., L. Wu, M. Egerton, A. Wilson, K. Shortman, and R. Scollay. 1989. A murine early thymocyte developmental sequence is marked by transient expression of the interleukin 2 receptor. *Proc. Natl. Acad. Sci. USA.* 86:1614.
43. Trowbridge, I.A., J. Lesley, J. Trotter, and R. Hyman. 1985. Thymocyte subpopulation enriched for progenitors with an unrearranged T cell receptor β chain gene. *Nature (Lond.).* 315:666.
44. Crispe, I.N., and M.J. Bevan. 1987. Expression and functional significance of the J11d marker on mouse thymocytes. *J. Immunol.* 138:2013.
45. Crispe, I.N., M.W. Moore, L.A. Husmann, L. Smith, M.J. Bevan, and R.P. Shimonkevitz. 1987. Differentiation potential of subsets of $CD4^-8^-$ thymocytes. *Nature (Lond.).* 329:336.
46. Raulet, D.H. 1989. The structure, function, and molecular genetics of the γ/δ T cell receptor. *Annu. Rev. Immunol.* 7:175.
47. Yagita, H., T. Nakamura, J. Asakawa, H. Matsuda, S. Tansyo, Y. Iigo, and K. Okumura. 1989. CD2 expression in murine B cell lineage. *Int. Immunol.* 1:94.
48. Sen, J., N. Rosenberg, and S.J. Burakoff. 1990. Expression and ontogeny of CD2 on murine B cells. *J. Immunol.* 144:2925.
49. Mombaerts, P., J. Iacomini, R.S. Johnson, K. Herrup, S. Tonegawa, and V.E. Papaioanou. 1992. RAG-1 deficient mice have no mature B and T lymphocytes. *Cell.* 68:869.
50. Spangrude, G.J., C.E. Muller-Sieburg, S. Heimfeld, and I.L. Weissman. 1988. Two rare populations of mouse $Thy1^{lo}$ bone marrow cells repopulate the thymus. *J. Exp. Med.* 167:1671.
51. Kuziel, W.A., J. Lewis, J. Nixon-Fulton, R.E. Tigelaar, and P.W. Tucker. 1991. Murine epidermal γ/δ T cells express Fcγ receptor II encoded by the FcγRα gene. *Eur. J. Immunol.* 21:1536.
52. Foy, T.M., R.G. Lynch, and T.J. Waldschmidt. 1992. Ontogeny and distribution of the murine B cell FcγRII. *J. Immunol.* 149:1516.
53. Titus, J.A., F.D. Finkelman, D.A. Stephany, J.F. Jones, and D. Segal. 1984. Quantitative analysis of Fcγ receptors on murine spleen cell populations by using dual parameter flow cytometry. *J. Immunol.* 133:556.
54. Ravetch, J.V., and J.-P. Kinet. 1991. Fc receptors. *Annu. Rev. Immunol.* 9:457.
55. Huesmann, M., B. Scott, P. Kisielow, and H. von Boehmer. 1991. Kinetics and efficacy of positive selection in the thymus of normal and T cell receptor transgenic mice. *Cell.* 66:533.
56. Schatz, D.G., M.A. Oettinger, and M.S. Schlissel. 1992. V(D)J recombination: molecular biology and regulation. *Annu. Rev. Immunol.* 10:359.
57. Alt, F.W., E.M. Oltz, F. Young, J. Gorman, G. Taccioli, and J. Chen. 1992. V(D)J recombination. *Immunol. Today.* 13:306.
58. Bosma, M.J., and A.M. Carroll. 1991. The SCID mouse mutant: definition, characterization and potential uses. *Annu. Rev. Immunol.* 9:323.
59. Groettrup, M., A. Baron, G. Griffiths, R. Palacios, and H. von Boehmer. 1992. T cell receptor (TCR) β chain homodimers on the surface of immature but not mature α, γ, δ chain deficient T cell lines. *EMBO (Eur. Mol. Biol. Organ.) J.* 11:2735.
60. Mombaerts, P., A.R. Clarke, M.A. Rudnicki, J. Iacomini, S. Itohara, J.J. Lafaille, L. Wang, Y. Ichikawa, R. Jaenisch, M.L. Hooper, and S. Tonegawa. 1992. Mutations in T cell antigen receptor genes α and β block thymocyte development at different stages. *Nature (Lond.).* 360:225.
61. Shinkai, Y., S. Koyasu, K.-I. Nakayama, K.M. Murphy, D.Y. Loh, E.L. Reinherz, and F.W. Alt. Restoration of T cell development in RAG-2 deficient mice by functionally rearranged TCR transgenes. *Science (Wash. DC).* 259:822.
62. Ra, C., M.-H.E. Jouvin, U. Blank, and J.-P. Kinet. 1989. A macrophage Fcγ receptor and mast cell receptor for IgE share an identical subunit. *Nature (Lond.).* 341:752.
63. Lanier, L.L., G. Yu, and J.P. Philips. 1989. Co-association of CD3ζ with a receptor (CD16) for IgG Fc on human NK cells.

Nature (Lond.). 342:803.

64. Anderson, P., M. Caliguiri, M. O'Brien, C. Manley, J. Ritz, and S.F. Schlossman. 1990. FcγRIII (CD16) is included in the ζ NK receptor complex expressed by human natural killer cells. *Proc. Natl. Acad. Sci. USA.* 87:2274.
65. Moingeon, P., J.L. Lucich, D.J. McConkey, F. Letourneur, B. Malissen, J. Kochan, H.-C. Chang, H.-R. Rodewald, and E.L. Reinherz. 1992. CD3ζ dependence of the CD2 pathway of activation in T lymphocytes and natural killer cells. *Proc. Natl. Acad. Sci. USA.* 89:1492.
66. Kato, K., M. Koyanagi, H. Okada, T. Takanashi, Y.W. Wong, A.N. Barclay, A.F. Williams, K. Okumura, and H. Yagita. 1992. CD48 is a counter-receptor for mouse CD2 and involved in T cell activation. *J. Exp. Med.* 176:1241.